

# UC Office of the President

## Recent Work

### Title

Adenosine A2a receptors form distinct oligomers in protein detergent complexes

### Permalink

<https://escholarship.org/uc/item/9wq0h1n3>

### Authors

O'Malley, Michelle Ann  
Schonenbach, Nicole S  
Rieth, Monica D  
[et al.](#)

### Publication Date

2016-08-20

### Data Availability

The data associated with this publication are within the manuscript.

Peer reviewed

Received Date : 10-Jul-2016

Revised Date : 10-Aug-2016

Accepted Date : 15-Aug-2016

Article type : Research Letter

## **Adenosine A2a receptors form distinct oligomers in protein detergent complexes**

### **Author List**

Nicole S. Schonenbach<sup>a</sup>, Monica D. Rieth<sup>a</sup>, Songi Han<sup>a, b</sup>, Michelle A. O'Malley<sup>a\*</sup>

### **\*Correspondence To**

M.A. O'Malley, Department of Chemical Engineering, University of California Santa Barbara, Engineering II, Room 3357 Mail Code 5080, Santa Barbara, CA 93106. Tel: 1(805)-893-4769, FAX: 1(805)893-4713 Email: momalley@engineering.ucsb.edu

### **Affiliations**

<sup>a</sup> Department of Chemical Engineering, University of California Santa Barbara, Engineering II, Room 3357 Mail Code 5080, Santa Barbara, CA 93106

<sup>b</sup> Department of Chemistry and Biochemistry, University of California Santa Barbara, Mail Code 9510, Santa Barbara, CA, 93106-9510

### **Email Addresses**

NSS: nicole\_schonenbach@engineering.ucsb.edu, MDR: mdrieth12@engineering.ucsb.edu, SH: songi@chem.ucsb.edu, MAO: momalley@engineering.ucsb.edu

**Author Contributions:** NSS, MAO and SH designed the experiments. MAO and SH supervised the study. NSS and MDR performed experiments and NSS carried out data analysis. NSS, SH, and MAO wrote and revised the manuscript.

This article has been accepted for publication and undergone full peer review but has not been through the copyediting, typesetting, pagination and proofreading process, which may lead to differences between this version and the Version of Record. Please cite this article as doi:

10.1002/1873-3468.12367

This article is protected by copyright. All rights reserved.

## Abstract

The human adenosine A2a receptor (A2aR) tunes its function by forming homo-oligomers and hetero-oligomers with other GPCRs, but the biophysical characterization of these oligomeric species is limited. Here, we show that upon reconstitution into an optimized mixed micelle system, and purification via an antagonist affinity column, full length A2aR exists as a distribution of oligomers. We isolated the dimer population from the other oligomers via size exclusion chromatography and showed that it is stable upon dilution, thus supporting the hypotheses that the A2aR dimer has a defined structure and function. This study presents a crucial enabling step to a detailed biophysical characterization of A2aR homodimers.

**Keywords:** G protein-coupled receptor (GPCR), dimer, oligomer, size exclusion chromatography (SEC), protein detergent complex (PDC), ligand chromatography

## Highlights

- Full length adenosine A2a receptor forms multiple oligomers *in vitro*
- Oligomer species can be separated by size exclusion chromatography
- Separated A2aR dimers are stable and do not redistribute into mixed populations

## Introduction

G protein-coupled receptors (GPCRs) are integral membrane proteins that trigger highly specific cellular responses to subtle environmental cues<sup>1</sup>. Localized at the cell surface, they are easily accessible to extracellular therapeutics that activate or inhibit associated intracellular reaction cascades, making them ideal pharmaceutical targets<sup>2</sup>. The motivation for this study is rooted in increasing evidence that many GPCRs tune their function by forming homo- or heteromeric oligomer complexes, spurring the development of novel therapeutics tailored to associate with specific oligomers<sup>3, 4</sup>. However, experimental difficulties stemming from low overall abundance<sup>5</sup>, dynamic flexibility<sup>6</sup>, and poor stability in membrane mimetic systems<sup>7-9</sup> have hindered biophysical insight into the stability and structure-function of membrane protein oligomers, especially that of GPCRs.

The human adenosine A2a receptor (A2aR) is an excellent candidate for piloting new tools that decipher oligomer structure-function of isolated, reconstituted GPCRs, as it is highly expressed in heterologous microbial systems<sup>10-12</sup>, forms oligomers in mammalian membranes<sup>13</sup>, and several crystal structures of A2aR variants are available<sup>14-20</sup>. There is an extensive body of literature motivating the functional relevance of A2a-containing homo- and hetero-dimers, and their role in central nervous system disorders<sup>21-25</sup>. It has also been suggested that A2aR homo-dimers<sup>13</sup> or even higher order homo-oligomers<sup>26</sup> are the functional unit at the mammalian plasma membrane and a main component of hetero-oligomer formation<sup>27-29</sup>. However, the functional significance of A2aR homo-oligomers remains unclear, as the monomeric form is still capable of binding extracellular ligand<sup>16, 30, 31</sup>. Similarly, the monomers of other homo-oligomer forming Class A GPCRs, such as rhodopsin and the  $\beta$ 2-adrenergic receptor, are capable of binding ligand and activating their respective G proteins on their own<sup>32-34</sup>. Therefore, studies of isolated A2aR monomer and oligomers would lend critical insight into the role of self-association.

Even though several crystal structures of A2aR variants are available<sup>14-20</sup> that provide valuable insight into the ligand binding pocket and putative oligomeric interfaces<sup>19, 35</sup>, each structure provides only a single snapshot of one of several dynamic receptor conformations. It is critical to note that all A2aR crystal structures solved to date are C-terminally truncated variants, with A2aR's unusually long and disordered tail (122 amino acids) removed to facilitate crystallography measurements. However, the C-terminus likely plays an important role in mediating oligomer formation and stability as its presence is known to impact the distribution of monomers and homo-dimers at the cell surface<sup>36</sup>. Reportedly, the C-terminus of A2aR also interacts electrostatically with the third cytoplasmic loop of the dopamine D2 receptor<sup>37</sup>. Therefore, characterization of the full length, wild-type A2aR is important for the study of any

A2aR containing oligomers. Biophysical techniques such as fluorescence resonance energy transfer (FRET)<sup>38</sup>, surface plasmon resonance (SPR)<sup>39, 40</sup>, and electron paramagnetic resonance (EPR)<sup>41-44</sup> can complement crystallographic data by providing information about structural dynamics and inter-protomer distances of membrane protein oligomers. These biophysical tools are not principally limited by protein size, or the presence of a disordered protein region, such as the C-terminal tail of A2aR, permitting investigations into the role of such termini in oligomer formation and protein function.

This study presents a strategy to produce, reconstitute, and purify full length human A2aR homo-oligomers for biophysical studies from the yeast *Saccharomyces cerevisiae*. A2aR homo-dimer is enriched and isolated from the monomer and higher-order oligomeric species via a tandem two-step affinity chromatography approach, followed by size exclusion chromatography (SEC). We find that wild type A2aR distributes into discrete oligomeric states upon purification and micellar reconstitution, of which A2aR homo-dimers, in particular, are a distinct and stable species. We also find that some, but not all, modifications in the C-terminus disrupt the A2aR homo-dimer stability, suggesting that the C-terminus plays an important role in mediating the oligomerization propensity of A2aR. The isolation of stable A2aR dimers is an important first step towards the study of structure-function relationships of A2aR's various oligomeric species.

## Materials and Methods

### *Cloning, Protein Expression and Purification*

Full length human adenosine A2a receptor (A2aR) was cloned into an expression cassette containing a GAL1,10 promoter, a synthetic pre-pro leader peptide<sup>45</sup> and a C-terminal 10 histidine tag within the yeast integrating pITy vector<sup>46</sup>, provided by the lab of Anne Robinson at Tulane University. Standard PCR techniques were used to amplify wild type A2a from pcDNA 3.1 + vectors from Missouri S&T cDNA. A mutant receptor containing a C-terminal cysteine to serine (C394S) substitution was created by splice overlap extension (SOE) PCR<sup>47</sup>, with primers reported in Table S1. Vector constructs containing A2aR were linearized and chemically transformed into *S. cerevisiae* strain BJ5464 (MAT $\alpha$  ura3-52 trp1 leu2 $\Delta$ 1 his3 $\Delta$ 200 pep4::HIS3 prb1 $\Delta$ 1.6R can1 GAL) (provided by the lab of Anne Robinson at Tulane University) using a high efficiency lithium acetate method<sup>48</sup>. Transformants were screened for expression via SDS-PAGE and Western blot analysis described below.

Receptor was purified and solubilized in micelles following previously described protocols<sup>49</sup>. Briefly, 50 mL cultures were grown overnight in YPD (1% yeast extract, 2% peptone, and 2% dextrose) to at least 10 OD and were induced by centrifuging cells and removing YPD before resuspending cells in YPG medium (1% yeast, 2% peptone, and 2% D-galactose) at an initial OD of 0.5. A2aR was expressed for 24 hours at 30 °C with shaking at 250 rpm. Cells were harvested by centrifugation at 2,000  $\times$  g for 5 minutes, washed in sterile PBS buffer and centrifuged again before storage at -80°C until needed for protein preparation. Cells were lysed using mechanical bead lysis carried out with 10 mL 0.5 mm zirconia silica beads (BioSpec, #11079105z), 10 mL of lysis buffer (50mM sodium phosphate, 300 mM sodium chloride, 10% v/v glycerol, pH = 8.0) containing 2% (w/v) n-Dodecyl- $\beta$ -D-maltopyranoside

(DDM), 1% (w/v) 3-[(3-Cholamidopropyl)dimethylammonio]-1-propanesulfonate (CHAPS), and 0.2% (w/v) cholesteryl hemisuccinate (CHS) (Anatrace, Maumee, OH #D310, C216, CH210, respectively) and an appropriate quantity of 100X Pierce Halt EDTA-free protease inhibitor #78439) per 100 mL of culture. Un-lysed cells and cell debris were pelleted by centrifugation at  $3,220 \times g$  for 10 minutes and  $8,000 \times g$  for 30 minutes, respectively, and solubilized protein was incubated with Nickel NTA resin (Pierce, #88221) resin overnight. After extensive washing in purification buffer (50 mM sodium phosphate, 300 mM sodium chloride, 10% (v/v) glycerol, 0.1% DDM, 0.1% CHAPS and 0.2% CHS, pH 8) and low imidazole concentrations (20-50 mM), protein was eluted into purification buffer containing 0.1% DDM, 0.1% CHAPS and 0.2% CHS and 500 mM imidazole. Prior to further chromatography purification and separation, imidazole was removed using a PD-10 desalting column (GE Healthcare, # 17085101). For experiments in which a paramagnetic label was attached to free cysteines, at least 10 molar excess of nitroxide radical MTSL (Toronto Chemicals, #0875000) was reacted with A2aR while bound to Ni NTA resin overnight, followed by extensive washing to remove unreacted spin label before elution described in greater detail in Supplemental Methods.

#### *SDS-PAGE and Western Blot Detection of A2aR*

Hand-casted 10% SDS-PAGE gels were prepared in BioRad Criterion empty cassettes (BioRad # 3459902, 3459903). Lysate control samples were prepared by lysing the equivalent of 5 OD cell pellets with 35  $\mu$ L YPER (Fisher Scientific, # 8990) at room temperature for 20-30 minutes before combining with equal volume 2 X Laemmli buffer (4% (w/v) SDS, 20% (v/v) glycerol, 120 mM Tris, pH 6.8) and solubilizing at 37°C for one hour. Purified protein samples

were prepared by mixing equal volumes of solubilized protein and 2X Laemmli buffer and incubating 37°C for 20 minutes. All samples were centrifuged  $4,000 \times g$  for 1 minute to pellet cell debris and minimize bubbles prior to loading 14  $\mu\text{L}$  (for 26-well gel) or 20 $\mu\text{L}$  (for 18-well gel) per lane. As a standard, 7 $\mu\text{L}$  of Magic Mark XP Western protein ladder (Thermo Scientific, product number LC5602) was run on each gel for approximate molecular weight determination. Electrophoresis was carried out for 90-100 minutes at 100 volts. Proteins were then transferred to 0.2  $\mu\text{m}$  nitrocellulose membranes (BioRad, # 170-4159) for Western blotting using a BioRad Transblot Turbo, mixed molecular weight protocol. Membranes were blocked in TBST containing 5% (w/v) dry milk, then probed with primary anti-A2a antibody mapping to the third intracellular loop (Santa Cruz Biotechnology, # sc32261) 1:500 in TBST containing 0.5% milk. Imaging of the A2aR bands was facilitated by probing with a fluorescent DyLight 550 secondary antibody (Abcam, ab96880) at 1:600 in TBST containing 0.5% (w/v) milk.

#### *Ligand Affinity Chromatography Purification of Active A2aR*

Ligand affinity media was prepared as previously described to purify active A2aR<sup>11,50</sup>. In brief, eight milliliters of washed Affigel 10 resin (BioRad, # 1536099) was mixed with 48 milliliters of dimethylsulfoxide (DMSO) containing 24 mg of the high affinity ( $K_d = 32 \text{ nM}$ ) A2aR antagonist xanthine amine congener (XAC) (Sigma, product number X103) and mixed gently in an Erlenmeyer flask for 20 hours at room temperature. The amount of ligand bound to the resin was estimated to be 5.6  $\mu\text{mol/L}$  by measuring the absorbance of the XAC-DMSO solution before and after the reaction at 310 nm in 10 mM HCl and comparison to a standard curve. In order to quench the reaction, the resin was washed with several resin volumes of 50 mM Tris-HCl (pH = 7.4). The resin was then washed into 20% (v/v) ethanol and packed into a



Tricorn 10/50 empty column (GE Healthcare, Pittsburgh, PA) while connected to a BioRad Duoflow (BioRad, Hercules, PA). Once packed, the column contained approximately 4 milliliters of settled resin.

To purify active A2aR, the column was equilibrated thoroughly in 4 column volumes of purification buffer containing 50 mM sodium phosphate, 300 mM sodium chloride, (pH = 8), 10% (v/v) glycerol, 0.1% DDM, 0.1% CHAPS, 0.02% CHS. After desalting IMAC-purified receptor, the sample was diluted to 5.5 mL and applied to a 5 mL sample loop on a BioRad Duoflow FPLC which loaded the sample onto the column at a rate of 0.1 mL/min. Inactive receptor was washed from the column by flowing 10 mL of purification buffer at 0.2 mL/min, followed by 16 mL at 0.4 mL/min. Active receptor was eluted from the column by switching to purification buffer containing 20 mM of low affinity ( $K_d = 1.6 \mu\text{M}$ ) antagonist theophylline (Sigma, # T1633). Western blot analysis of 4 mL fractions indicated that a majority of A2aR was active, and typically eluted in the first 4 to 6 elution fractions. These 4 mL fractions were then pooled, concentrated through a 30 kDa molecular weight cutoff centrifugal filter (Millipore, # UFC803096) and passed through a PD-10 desalting column to remove the theophylline prior to size exclusion chromatography.

#### *Size Exclusion Chromatography*

Oligomeric species of solubilized A2aR were separated by injecting 250  $\mu\text{L}$  samples onto a prepacked Tricorn Superdex 200 10/300 GL column (GE Healthcare) connected to a BioRad Duoflow FPLC, and 0.5 mL fractions were collected with a BioFrac fraction collector. Prior to injecting samples, the column was fully equilibrated with at least 60 mL of running buffer (150mM sodium chloride, 50 mM sodium phosphate, 10% glycerol, 0.1% DDM, 0.1% CHAPS,

0.02% CHS, pH = 8) at a flow rate of 0.2 mL/min. If the column was pre-equilibrated, only 15 mL of running buffer was necessary to fluidize the bed for reproducible separations. Samples were eluted from the column in 30 mL of running buffer at the same flow rate. Fractions were analyzed for oligomeric state by SDS-PAGE and Western blot.

### *Size Exclusion Chromatography-coupled Multi-Angle Light Scattering*

Light scattering experiments were performed on 100  $\mu$ L solubilized receptor samples using a Wyatt Technology (Santa Barbara, CA) analytical size exclusion column (WTC-MP030S5) with the same buffer composition and flow rate as described for size exclusion chromatography (50 mM sodium phosphate, 150 mM sodium chloride, 10% glycerol, 0.1% DDM, 0.1% CHAPS, and 0.02% CHS pH = 8, 0.2 mL/min), connected to an Agilent 1200 Infinity Series HPLC. Wyatt Technologies miniDAWN TREOS light scattering detector and OptiLab TrEX refractive index detector were connected downstream of the Agilent 1200 variable wavelength detector. Data analysis was carried out using the protein conjugate analysis program within Wyatt's ASTRA V software (version 5.3.4). Briefly, the molecular weight of protein in a protein detergent complex (PDC) can be defined using the relationship in Equation 1 if the detergent absorbance at 280 nm is zero<sup>51</sup>.

$$M_{w,protein} = \frac{\Delta LS * \Delta UV_{280}}{K * \epsilon_{280,protein} (\Delta RI)^2} \quad \text{Equation 1}$$

In Equation 1, the difference in signal between the eluting sample and the running buffer from the light scattering detector ( $\Delta LS$ ), the ultraviolet absorbance (280 nm) detector ( $\Delta UV$ ), differential refractive index ( $\Delta RI$ ) are measured, K is a constant, and  $\epsilon_{280, protein} = 1183.5 \text{ mL} * \text{g}^{-1} * \text{cm}^{-1}$  is the mass extinction coefficient of A2aR, estimated by the protein primary sequence.

Accepted Article

Due to the required use of centrifugal concentration to concentrate A2aR, the mixed micelle solution in these samples contained CHAPS and CHS in sufficient quantities to warrant absorbance at 280 nm. However, this excess of detergent (e.g. empty micelles) eluted separately from protein-containing micelles (Figure S1) and thus a molar extinction coefficient of the detergent modifier was assumed to be zero for protein-containing absorbance peaks. Similar assumptions have been made previously for mixed micelles containing the same detergent components at different ratios<sup>52</sup>. The change in refractive index at 658 nm as a function of concentration (dn/dc) of A2aR was assumed to be 0.185 mL/g, a “consensus value” for protein dn/dc that is independent of amino acid composition<sup>53</sup> and of the mixed micelle solution was estimated to be 0.183, based on calculation of the correct molecular weight (39.8 kDa)<sup>54</sup> over the elution peak of empty micelles (Figure S2).

## Results and Discussion

### *Purified A2aR Distributes into a Mixture of Putative Oligomer Species*

Full length A2a with a C-terminal 10 histidine tag (A2aR) was overexpressed in *S. cerevisiae* and purified using a combination of immobilized nickel metal affinity (IMAC) and a custom synthesized ligand affinity column, as illustrated in Figure 1. The C-terminus of A2aR is susceptible to proteolytic cleavage<sup>50</sup>, and as such IMAC purification via the 10 histidine tag resulted in purification of both full length A2aR and C-terminal fragments. A custom ligand affinity column (described in *Materials and Methods*) was implemented to remove any C-terminal cleavage products and purify only full length, "active" A2aR from this IMAC eluted mixture. Here, we have described “active” receptor as properly folded A2aR capable of binding to the high affinity xanthine amine congener (XAC) antagonist affixed to resin. Previously, an

Accepted Article

optimized mixed micelle composition for the stabilization of active A2aR was determined to contain DDM, CHAPS, and CHS at a mass ratio of CHAPS and CHS to all surfactant ( $\delta$ ) of 0.55<sup>8</sup>. Small angle neutron scattering (SANS) measurements determined that this particular micelle composition provides a micelle thickness approximately the same as that of a lipid bilayer, while also demonstrating that micelle geometry is not the only factor in GPCR stabilization, but cholesterol content also influences A2aR activity *in vitro*<sup>54</sup>. Ligand affinity purification of A2aR confirmed that the majority of A2aR purified with this mixed micelle system was "active", as determined by Western blot analysis of fractions eluted from the ligand affinity column in Figure 2. As indicated in Figure 2A, both a putative monomer and a putative dimer band were observed in the elution fractions containing a high excess of theophylline (20mM), suggesting a mixture of oligomeric populations resulting from yeast membrane solubilization. Interestingly, when a mutant receptor substituting the lone C-terminal cysteine with a serine (C394S) was purified by ligand affinity (Figure 2B) two notable differences from the wild type receptor arose: 1) while ~80% of C394S A2aR eluted as active receptor, there was a notable increase in the amount of protein that eluted as inactive receptor, and 2) C394S A2aR ran primarily as monomer on SDS-PAGE, suggesting that the dimer forming propensity or stability is reduced by the C394S modification.

Still, it is difficult to determine the oligomeric content from this observation alone, as SDS-PAGE is capable of breaking apart weakly associated oligomers, and the amount of detergent bound to membrane proteins influences their migration through acrylamide gels<sup>55</sup>. However, from this analysis we hypothesized that A2aR eluted from the ligand affinity column constituted a mixture of oligomeric species, and the stability of the dimer species is weakened by the substitution of the C-terminal cysteine. It is also possible that ligand binding alters the

oligomer population and distribution, as suggested by *in vivo* experiments within mammalian cell lines<sup>13, 56</sup>. For instance, findings from Canals and coworkers suggests incubation of A2aR-overexpressing HEK cells with the potent agonist CGS-21680 leads to the formation of receptor clusters, yet does not affect the degree of dimerization<sup>13</sup>. However a later study indicated that the same agonist increases A2a homodimerization, while antagonists caffeine and SCH58261 reduce the population of homodimers<sup>56</sup>. In either case, size exclusion chromatography was employed to more directly query the population and distribution of oligomeric states in mixed micelles, as well as to assess any relative impact from antagonist binding.

#### *Size Exclusion Chromatography Estimates Purified A2aR Oligomeric States*

Size exclusion chromatography (SEC) was applied to A2aR eluted from the antagonist affinity column to identify and separate oligomeric states that are stabilized by this protein detergent complex. Fractions of ligand-purified A2aR were concentrated and applied to a desalting column to remove theophylline before application to a Superdex 200 10/300 GL column to separate the various oligomer species present. For the wild type A2aR, three oligomer species were consistently observed, as well as a fourth peak that corresponded to empty micelles, as illustrated in Figure 3A. A higher order, possibly aggregated, oligomeric state was observed to elute first. The relative quantity of this aggregate species compared to other oligomeric states varied from preparation to preparation, as shown in supplementary Figure S3. However, experimental evidence indicates that this high molecular weight population is not exclusively misfolded, or merely a product of centrifugal concentration, as it was present in sample directly taken from ligand affinity column elution without any concentration or desalting steps (Figure S4).

Distinct dimer and monomer species were not only observed for the wild type receptor, but were clearly separated via size exclusion, indicating that structural and functional studies on specific oligomeric states are possible in micelles (Figure 3A). However, purification by SEC dilutes protein sample below the threshold concentration necessary to perform many biophysical analyses (50-100  $\mu$ M), and further concentration of these samples is likely needed. As such, the effect of centrifugal concentration on the dimer state was explored as described below. The SEC purification of active C394S A2aR revealed that the primary eluting species was a monomer population (Figure 3B). The difference in oligomer species observed for wild type and C394S A2a indicates a possible dimer stabilizing effect of the C394 residue by disulfide bond formation *in vitro*. Incubation of both wild type and C394S A2aR with 5 mM DTT revealed a higher molecular weight shift of the dimer species observed on SDS-PAGE compared with non-reduced samples (Figure S5). It is also important to note that this observed shift in molecular weight could be attributed to the breakage of four functionally important disulfide bonds between cysteines in the extracellular loops of A2aR<sup>49, 57, 58</sup>.

To further investigate the role of C394 in A2aR oligomerization *in vitro*, we investigated the effect of modifying the thiol on C394 without performing mutagenesis by attaching a paramagnetic spin label to the free cysteine. Such modification resulted in an SEC elution profile exhibiting the same oligomer species as unmodified wild type A2aR. Electron paramagnetic resonance (EPR) measurements displayed a significantly increased spin concentration per protein for wild type A2aR compared to C394S A2aR and distinct differences in their spectral lineshape, as discussed further in Supplemental Methods, Figure S7. Moreover, the EPR spectral lineshape of spin labeled wild type A2aR is characteristic of that of spin labels tethered to a solvent-exposed site, in contrast to the much more immobile features seen with spin labeled C394S

A2aR. This result strongly suggests that the dimer species observed in wild type A2aR is not an artefact of an artificial disulfide bond forming between C394 residues of nearby A2aR monomers, in which case the intensity and lineshape of spin labeled wild type A2aR and of C394S A2aR should have been comparable, as the majority of MTSL label detected would be bound to more constrained cysteine residues within the TM domains. The observation that a C394S A2aR binds less efficiently to the antagonist affinity column, together with the decreased dimer stability, implies that the specific C394 residue is somehow critical in stabilizing oligomers. This motivates further *in vitro* studies to unravel the underlying molecular and structural basis of this finding.

The chromatogram peak identified as “empty micelles” was verified by preparing sample of the same buffer containing the mixed micelle components lacking protein, and applying the same centrifugal concentration and desalting procedures to these mock prepared samples; a peak of similar intensity was observed in the same location for each SEC chromatogram (Figure S1). Unfortunately, the simultaneous concentration of detergent micelles during centrifugal concentration of membrane proteins is unavoidable, and is a common drawback in membrane protein purification. Thus, such trial-to-trial uncertainty is common and can lead to irreproducible measurements if subsequent analytical methods are sensitive to solvent composition<sup>59</sup>. Nevertheless, here we have shown that for A2aR reconstituted in mixed micelles, any excess empty micelles can be separated from A2aR-containing oligomeric species; this introduces a point of control for downstream characterization, especially for biophysical methods hampered by excess detergent micelles.

Surfactant binds to solubilized receptors and affects both the apparent molecular weight of the species (mass) and the receptor's hydrodynamic radius (size), thereby negating the ability to estimate accurate molecular weights of eluting species by comparing to SEC standards. We therefore employed multi-angle light scattering (MALS) to estimate molecular weights of the separated wild type species. SEC coupled to MALS is a powerful technique to measure the amount of light scattered by molecules eluting from a size exclusion column. By coupling concentration measurements from UV and refractive index detectors, the molecular weight of a protein (oligomer) in a PDC can be determined. SEC-MALS analyses of wild type A2aR (Figure 4) purified by ligand affinity chromatography determined the approximate molecular weights of the putative monomer and dimer to be 49.5 kDa and 109.2 kDa, respectively, and 332.3 kDa for the higher order oligomer species (Table 1). These calculations compare well with the expected molecular weight of A2aR monomer (46.8 kDa), dimer (93.6 kDa) and a heptamer higher-order species (327.6 kDa). No previous literature has directly indicated a functionally relevant A2aR heptamer, however its presence in active wild type A2aR sample that was not subjected to any concentration or desalting steps indicates that it can be stabilized and is worthwhile for future investigations. Recent findings in neuronal tissues suggest that A2aR forms higher order oligomers, further motivating these studies<sup>26</sup>. However, biophysical tools to characterize such higher order oligomerization are rare and difficult to implement<sup>60</sup>.

#### *A2aR Dimer is Stable upon Dilution*

To assess the stability of A2aR oligomers and concentration dependence, purified dimers were re-analyzed on an SEC column to assess their potential for re-distribution into multiple oligomer states. Protein oligomers *in vitro* are often thought to be in equilibrium with the



monomer or other oligomer states, as their distribution frequently depends on a range of factors including protein concentration, protein stability, lipid/membrane environment, detergent concentration, and the strength of the oligomer interaction.<sup>61</sup> While SEC can achieve separation of oligomers, if the oligomeric state is strongly dependent on the protein concentration, a thermodynamic equilibrium may favor a redistribution of an isolated oligomer species into a mixed population of oligomers before further studies can be performed. Here, we found that heavily diluted dimer (20x) from SEC elution remained a dimer, with little to no redistribution into other oligomeric states (Figure 5, Dimer (b)). Additionally, when multiple dimer fractions were pooled and concentrated using a centrifugal concentrator (30 kDa MW cutoff) to a volume ~1/3 of the initial sample volume, the majority of the protein (~86%) remained a dimer as estimated by integration of the UV absorbance trace over the protein containing peaks. However, a small amount of higher order oligomer/aggregate was also enriched during concentration, amounting to ~14% of the total eluted protein in this sample, consistent with higher-order oligomer enrichment during centrifugal concentration. Additionally, an “empty micelle” peak appeared upon concentration of dimer, which is consistent with previous observations. This increase in surfactant concentration during the centrifugal protein concentration step is a feature that hampers all structural studies of membrane proteins solubilized in detergent micelles.<sup>62</sup> However, by carrying out all downstream experiments on samples of equal volume, better control of surfactant concentration can be achieved. Our results demonstrate that the wild type A2aR dimer is stable for at least 3 days after being separated from other oligomer species, independent of detergent and protein concentration, which provides sufficient time for further downstream analyses. This implies that dimer formation is a protein-intrinsic property of A2aR, not a property imposed by the solution environment. This information is especially valuable for

studies that seek to characterize the structure and dynamics of the dimer interface. Of the twelve crystal structures, only one has captured a possible oligomer interface<sup>19</sup>, which does not agree with previous attempts to elucidate the A2a dimer structure<sup>35, 63, 64</sup>; thus, further experiments are necessary to determine whether this is a physiologically relevant interface or a product of thermostabilizing mutations and non-native crystallization conditions.

## Conclusions

We have shown that the full length, wild type adenosine A2aR forms multiple distinct oligomer species in an optimized mixed micelle system, and that these oligomers can be separated from each other by size exclusion chromatography in preparation for biophysical characterization. Although difficult to work with, owing to its long and unstable C-terminus, our analysis of solubilized A2aR infers that the receptor adopts multiple, stable oligomer species in contrast to other structural studies of A2aR<sup>30</sup>. The C-terminal cysteine (C394) appears to promote dimer stabilization of A2aR *in vitro*, without which most purified A2aR in this system exists as monomer in mixed micelles, a feature which can be exploited to control oligomer state for biophysical study. Furthermore, we present evidence that the wild type dimer is not artificially crosslinked by neighboring C394 residues, as “blocking” of the free thiol with a paramagnetic spin label results in SEC separation of the same oligomer populations as an unmodified receptor. EPR spectral lineshape analysis of the spin labeled wild type A2aR moreover demonstrates that a significant fraction of C394 is available for spin labeling and is solvent-exposed. This suggests that it is obligatory to study the full length A2aR with the intact C-terminus in order to investigate the structure-function relationship of A2aR oligomerization. To develop novel therapeutics that target A2a homodimers, the task remains to link structural

features of these multimers to receptor function and signaling<sup>65</sup>. In particular, oligomer interfaces, inter-protomer distances, dynamics, and orientation of ligand binding pockets of separated species will provide crucial information for determining ligand linker lengths and chemical interactions between oligomers and ligands. As this field advances closer to elucidating the structure-function relationship of GPCR oligomers, there is further motivation to investigate structural dynamics upon ligand binding, as changes in the oligomer interface upon activation have been detected for other GPCR homodimers including the dopamine D2<sup>66</sup> and metabotropic glutamate mGluR5<sup>67</sup> receptors among others. While the quantity of A2aR dimer and the presence of the highly disordered C-terminus in this study hinders crystallographic experiments and traditional NMR measurements, other biophysical techniques such as EPR and FRET are now readily accessible for monomer and homo-dimer characterization. Our work represents a vital step toward characterizing the A2aR homodimer structure-function and dynamics *in vitro*, which can be extended to include hetero-oligomers or higher order homo oligomers of A2aR.

#### **Acknowledgements:**

The authors gratefully acknowledge funding support from the University of California Cancer Research Coordinating Committee Award number 597608-34384, the American Heart Association Award Number 14GRNT18690063, Hellman Faculty Fellowship number 44250-41844, a National Science Foundation Graduate Research Fellowship to NSS and the National Institute of General Medical Sciences of the National Institutes of Health under Award Number 1R01GM116128-01. The content is solely the responsibility of the authors and does not necessarily represent the official views of the National Institutes of Health. The pITy expression vector and *S. cerevisiae* BJ5464 strain were generously provided by Prof. Anne Robinson's lab at

Tulane University. The authors also thank Dr. Sophia Kenrick and Dr. Jason Lin at Wyatt Technology for guidance with light scattering experiments and Dr. Sunyia Hussain for thoughtful discussions.

### List of Tables:

**Table 1: Molecular weight determination of A2aR oligomers by SEC-MALS**

Oligomer Species	Predicted MW (kDa)	Calculated MW (kDa)	% Error
Monomer	46.8	49.5 (4%)	5.8
Dimer	93.6	109.2 (3%)	16.7
7-mer	327.6	332.3 (8%)	1.4

The relative standard deviation of the calculated molecular weight is shown in parentheses.

### List of Figures:

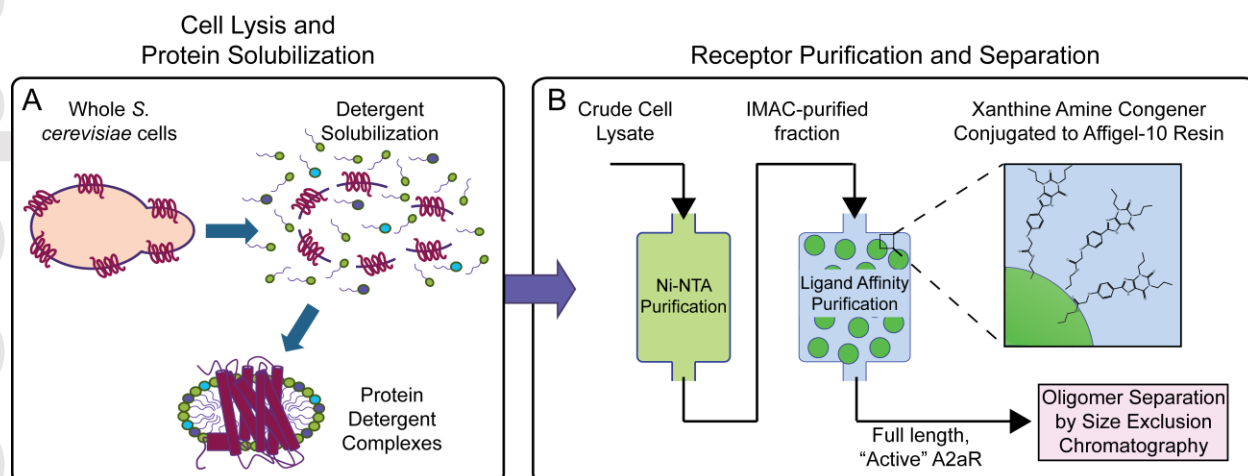


**Figure 1: GPCR Oligomers are extracted from yeast lysate.** (A) Schematic of A2aR solubilization from whole cell lysate into protein detergent complexes. (B) Illustration of two-part protein purification strategy involving an immobilized metal affinity chromatography (Ni-NTA) step to purify A2aR by its 10 histidine tag followed by a ligand affinity chromatography step. The inset cartoon depicts a resin bead with xanthine amine congener (XAC) molecules covalently bound to the resin surface.

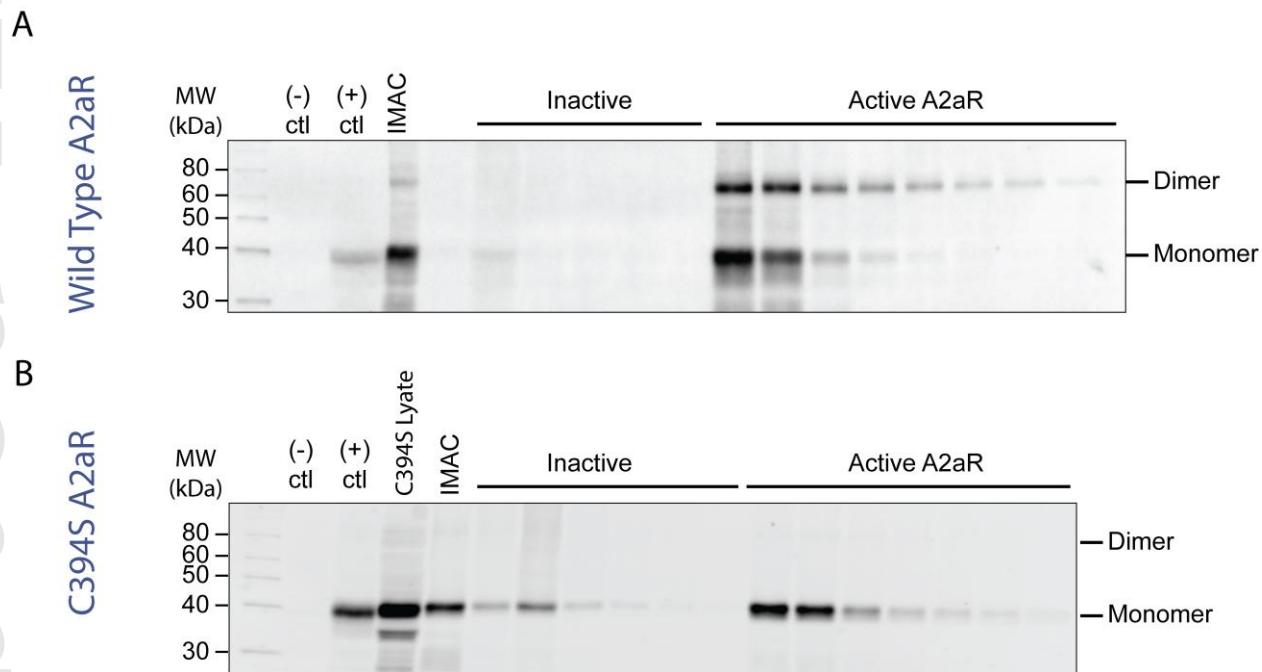


**Figure 2: An antagonist column separates solubilized A2aR that binds to ligand.** Affinity resin was covalently conjugated to high affinity antagonist xanthine amine congener (XAC,  $K_D = 32$  nM) and packed into an empty Tricorn 10/50 column for purification of full length “active” A2aR. Representative Western blots of elution fractions of wild type (A) and mutant C394S (B) A2aR from an antagonist affinity column. Each lane represents sample taken from 4 milliliter elution fractions collected. “Inactive” indicates receptor that does not bind to the column and elutes in the flow through. “Active” designates A2aR that associates with antagonist on the column, which is eluted when a high excess (20 mM) of low affinity theophylline supplemented to the column. Negative control (-) consists of 5 OD cell lysate of BJ5464 not expressing A2aR. Positive control ((+) ctl) consists of 5 OD cell lysate of BJ5464 after 24 hours of expression in YPG medium. IMAC indicates a semi-purified A2aR sample that has been eluted from Ni-NTA resin. A2aR was detected using primary antibody anti-A2a antibody (sc32261) and secondary

antibody DyLight 550 anti-Mouse (ab96880). Magic Mark protein ladder (LC5602) was used as the molecular weight standard.

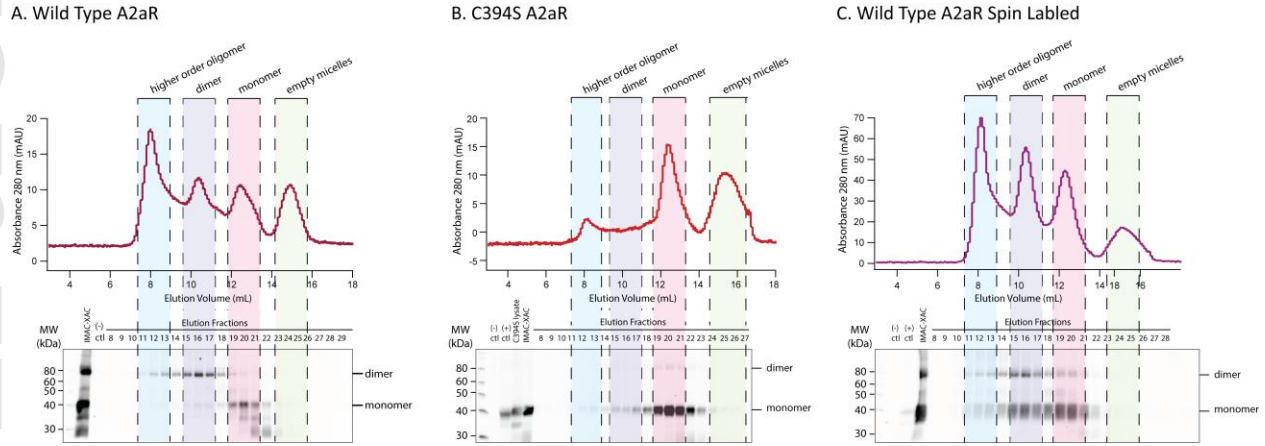


**Figure 3: Active A2aR oligomers are separated by size exclusion chromatography.** Size exclusion chromatogram and associated SDS-PAGE Western blot of purified full length wild type (A), mutant C394S (B), and spin labeled wild type (C). A2aR separates into distinct oligomer populations as indicated. Each lane on the Western blot represents a sample from 0.5 mL fractions eluted from a Superdex 200 10/300 GL (GE Healthcare) size exclusion column. The first peak appears at 7.5-9 mL and represents a higher order oligomer/aggregate peak. A dimer of wild type A2aR (A) and spin labeled wild type (C) elutes in a peak from 9.5-11 mL, which correlates with fractions 15-17 that run as primarily dimer around 80 kDa on SDS-PAGE. A peak in all three chromatograms from 11.5-13.5 mL correlates with fractions 19-21 that run primarily as monomer, at 40 kDa on SDS-PAGE. A light band appears at 30 kDa, which corresponds to late purification cleavage of A2aR C-terminus. In each Western blot, a negative control (-) consists of 5 OD cell lysate of BJ5464 not expressing A2aR. Positive control ((+) ctl) 5 OD cell lysate of BJ5464 expressing wild type A2aR in (B) and (C). “C394S lysate” indicates 5 OD lysate of BJ5464 expressing C394S A2aR. “IMAC-XAC” indicates purified active A2aR (wild type, C394S, or spin labeled wild type for A, B, and C, respectively). A2aR was detected using primary antibody anti-A2a antibody (sc32261) and secondary antibody DyLight 550 anti-Mouse (ab68890). Magic Mark protein ladder (LC5602) was used as the molecular weight standard in each case.

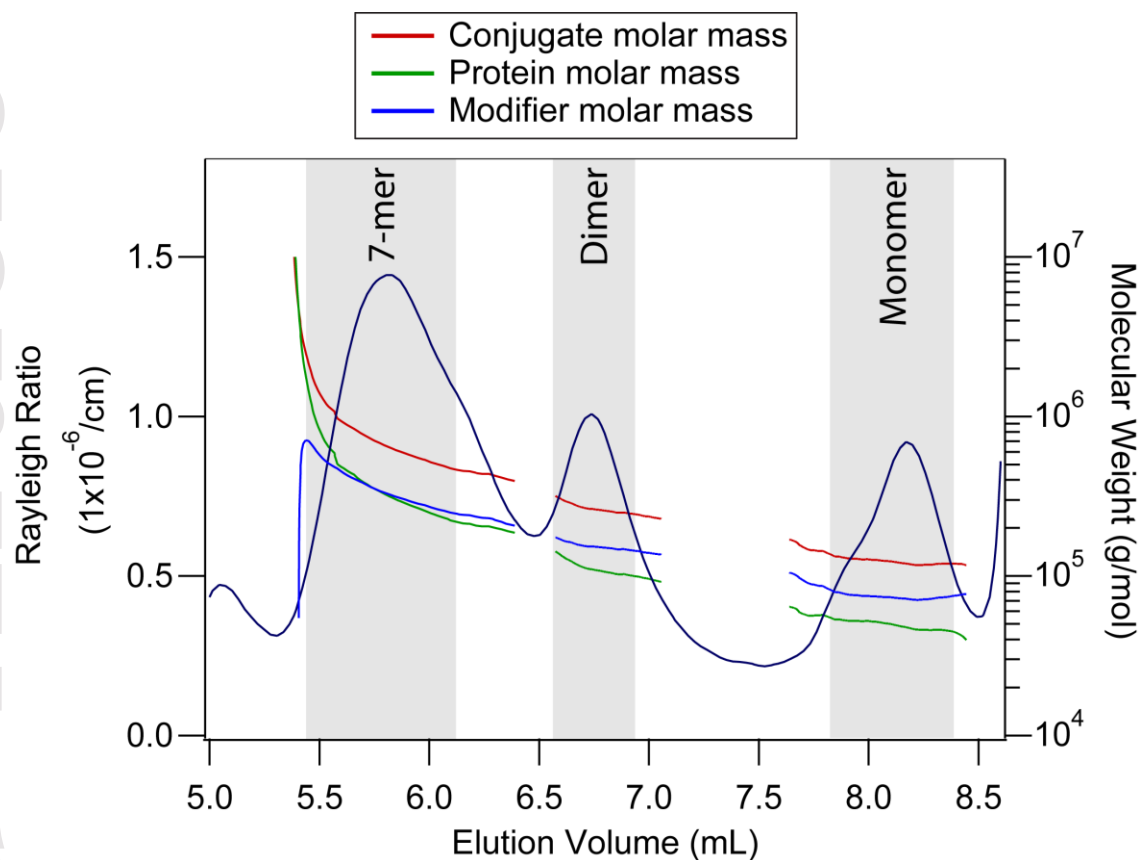


**Figure 4: Molecular weight of A2aR oligomers is determined by SEC-MALS.** Light scattering signal of the measured Rayleigh ratio (left axis, blue chromatogram) of elution of A2aR from a WTC-MP030S5 SEC column. The data were plotted with ASTRA software using a protein-conjugate analysis program and the following input values:  $dn/dc_{\text{protein}}=0.185$  (mL/g),  $dn/dc_{\text{surfactant}}=0.183$  (mL/g), and  $\epsilon_{\text{protein}}=1183.5$  mL/(g\*cm). The sample elution profile is representative of a 100  $\mu\text{L}$  injection of  $\sim 40\mu\text{M}$  A2aR onto a WTC-MP030S5 SEC column with a flow rate of 0.2 mL/min.

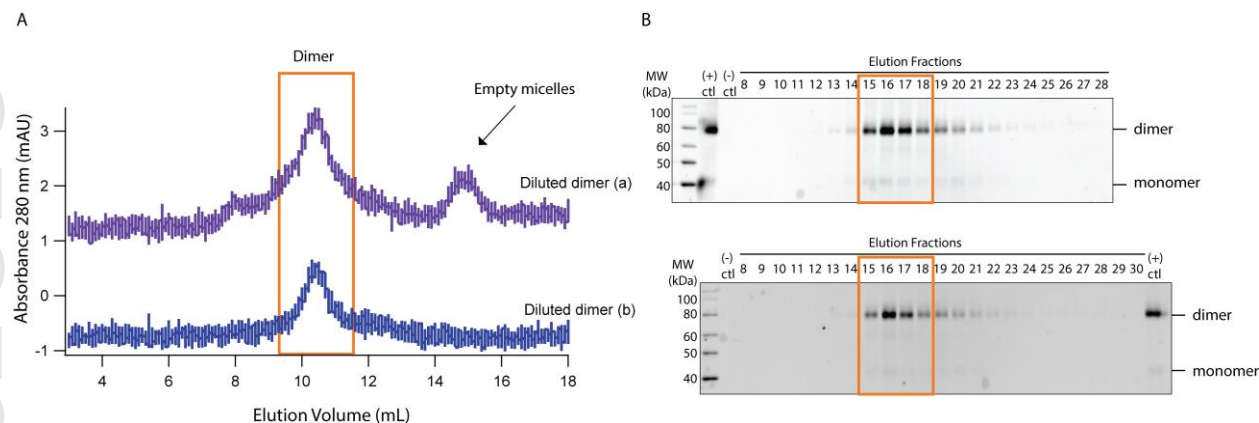


**Figure 5: A2aR dimers do not redistribute upon dilution.** (A) Chromatogram of samples “Diluted dimer” (a) and (b) on a Superdex 200 10/300 (GE Healthcare). Diluted dimer (a) indicates dimer fractions from one SEC separation, pooled together and concentrated to 1/3 of their initial volume, and injected onto the SEC column for a second consecutive separation. Diluted dimer (b) indicates a sample of the most concentrated fraction (16) from Figure 3 directly re-injected onto the SEC column. An orange box is drawn around the region which represents fractions 15-17 where ~66% of eluted protein is recovered, with a dilution factor of ~9. (B) Western blot analysis of the fractions collected from the size exclusion column for samples Diluted dimer (a) (lower) and Diluted dimer (b) (upper). Negative control is labeled (-) consists of 5 OD cell lysate of BJ5464 not expressing A2aR. Positive control ((+) ctl) contains the sample that was injected onto the column, prior to size separation. A2aR was detected using primary antibody anti-A2a antibody (sc32261) and secondary antibody DyLight 550 anti-Mouse (ab68890). Magic Mark protein ladder (LC5602) was used as the molecular weight standard.

## References

1. Bockaert J, Pin JP. Molecular tinkering of G protein-coupled receptors: an evolutionary success. *EMBO J* 1999, 18:1723-1729.
2. McNeely PM, Naranjo AN, Robinson AS. Structure-function studies with G protein-coupled receptors as a paradigm for improving drug discovery and development of therapeutics. *Biotechnology Journal* 2012, 7:1451-1461.
3. George SR, O'Dowd BF, Lee SP. G-protein-coupled receptor oligomerization and its potential for drug discovery. *Nat Rev Drug Discov* 2002, 1:808-820.
4. Schonenbach NS, Hussain S, O'Malley MA. Structure and function of G-protein coupled receptor oligomers: Implications for drug discovery. *WIREs Nanomedicine and Nanobiotechnology* 2015, 7:408-427.
5. Shire SJ, Shahrokh Z, Liu J. Challenges in the Development of High Protein Concentration Formulations. *Journal of Pharmaceutical Sciences* 2004, 93:1390-1402.
6. Vaidehi N. Dynamics and flexibility of G-protein-coupled receptor conformations and their relevance to drug design. *Drug Discov Today* 2010, 15:951-957.
7. Soubias O, Niu S, Mitchell DC, Gawrisch K. Lipid-Rhodopsin Hydrophobic Mismatch Alters Rhodopsin Helical Content. *Journal of American Chemical Society* 2008, 130:12465-12471.



8. O'Malley MA, Helgeson ME, Wagner NJ, Robinson AS. The morphology and composition of cholesterol-rich micellar nanostructures determine transmembrane protein (GPCR) activity. *Biophys J* 2011, 100:L11-13.
9. Milic D, Veprintsev DB. Large-scale production and protein engineering of G protein-coupled receptors for structural studies. *Front Pharmacol* 2015, 6:66.
10. Niebauer RT, Robinson AS. Exceptional total and functional yields of the human adenosine (A2a) receptor expressed in the yeast *Saccharomyces cerevisiae*. *Protein Expr Purif* 2006, 46:204-211.
11. O'Malley MA, Lazarova T, Britton ZT, Robinson AS. High-level expression in *Saccharomyces cerevisiae* enables isolation and spectroscopic characterization of functional human adenosine A2a receptor. *J Struct Biol* 2007, 159:166-178.
12. Wedekind A, O'Malley MA, Niebauer RT, Robinson AS. Optimization of the Human Adenosine A2a Receptor Yields in *Saccharomyces cerevisiae*. *Biotechnology Progress* 2006, 22.
13. Canals M, Burgueno J, Marcellino D, Cabello N, Canela EI, Mallol J, Agnati LF, Ferre S, Bouvier M, Fuxe K, et al. Homodimerization of adenosine A2a receptors: qualitative and quantitative assessment by fluorescence and bioluminescence energy transfer. *J Neurochem* 2004, 88:726-734.
14. Dore AS, Robertson N, Errey JC, Ng I, Hollenstein K, Tehan B, Hurrell E, Bennett K, Congreve M, Magnani F, et al. Structure of the adenosine A(2A) receptor in complex with ZM241385 and the xanthines XAC and caffeine. *Structure* 2011, 19:1283-1293.
15. Hino T, Arakawa T, Iwanari H, Yurugi-Kobayashi T, Ikeda-Suno C, Nakada-Nakura Y, Kusano-Arai O, Weyand S, Shimamura T, Nomura N, et al. G-protein-coupled receptor inactivation by an allosteric inverse-agonist antibody. *Nature* 2012, 482:237-240.
16. Jaakola VP, Griffith MT, Hanson MA, Cherezov V, Chien EY, Lane JR, Ijzerman AP, Stevens RC. The 2.6 angstrom crystal structure of a human A2A adenosine receptor bound to an antagonist. *Science* 2008, 322:1211-1217.
17. Lebon G, Edwards PC, Leslie AG, Tate CG. Molecular Determinants of CGS21680 Binding to the Human Adenosine A2A Receptor. *Mol Pharmacol* 2015, 87:907-915.
18. Lebon G, Warne T, Edwards PC, Bennett K, Langmead CJ, Leslie AG, Tate CG. Agonist-bound adenosine A2A receptor structures reveal common features of GPCR activation. *Nature* 2011, 474:521-525.
19. Liu W, Chun E, Thompson AA, Chubukov P, Xu F, Katritch V, Han GW, Roth CB, Heitman LH, AP IJ, et al. Structural basis for allosteric regulation of GPCRs by sodium ions. *Science* 2012, 337:232-236.
20. Xu F, Wu H, Katritch V, Han GW, Jacobson KA, Gao ZG, Cherezov V, Stevens RC. Structure of an agonist-bound human A2A adenosine receptor. *Science* 2011, 332:322-327.
21. Brugarolas M, Navarro G, Martinez-Pinilla E, Angelats E, Casado V, Lanciego JL, Franco R. G-protein-coupled receptor heteromers as key players in the molecular architecture of the central nervous system. *CNS Neurosci Ther* 2014, 20:703-709.
22. Ferre S, Ciruela F, Woods AS, Canals M, Burgueno J, Marcellino D, Karcz-Kubicha M, Hope BT, Morales M, Popoli P, et al. Glutamate mGlu5-Adenosine A2A-Dopamine D2 Receptor Interactions in the Striatum. Implications for Drug Therapy in Neuro-psychiatric Disorders and Drug Abuse *Current Medicinal Chemistry- Central Nervous System Agents* 2003, 3:1-26.
23. Ferre S, Quiroz C, Woods AS, Cunha R, Popoli P, Ciruela F, Lluís C, Franco R, Azdad K, Schiffmann SN. An Update on Adenosine A2a-Dopamine D2 Receptor Interactions: Implications for the Function of G Protein-Coupled Receptors. *Current Pharmaceutical Design* 2008, 14:1468-1474.
24. Torvinen M, Marcellino D, Canals M, Agnati LF, Lluís C, Franco R, Fuxe K. Adenosine A2A receptor and dopamine D3 receptor interactions: evidence of functional A2A/D3 heteromeric complexes. *Mol Pharmacol* 2005, 67:400-407.

25. Ciruela F, Gomez-Soler M, Guidolin D, Borroto-Escuela DO, Agnati LF, Fuxe K, Fernandez-Duenas V. Adenosine receptor containing oligomers: their role in the control of dopamine and glutamate neurotransmission in the brain. *Biochim Biophys Acta* 2011, 1808:1245-1255.
26. Vidi PA, Chen J, Irudayaraj JM, Watts VJ. Adenosine A(2A) receptors assemble into higher-order oligomers at the plasma membrane. *FEBS Lett* 2008, 582:3985-3990.
27. Ferre S. The GPCR heterotetramer: challenging classical pharmacology. *Trends Pharmacol Sci* 2015, 36:145-152.
28. Ferre S, Bonaventura J, Tomasi D, Navarro G, Moreno E, Cortes A, Lluís C, Casado V, Volkow ND. Allosteric mechanisms within the adenosine A-dopamine D receptor heterotetramer. *Neuropharmacology* 2015.
29. Fuxe K, Ferre S, Canals M, Torvinen M, Terasmaa A, Marcellino D, Goldberg SR, Staines W, Jacobsen KX, Lluís C, et al. Adenosine A2a and Dopamine D2 Heteromeric Receptor Complexes and Their Function. *Journal of Molecular Neuroscience* 2005, 26:209-219.
30. Bocquet N, Kohler J, Hug MN, Kusznir EA, Rufer AC, Dawson RJ, Hennig M, Ruf A, Huber W, Huber S. Real-time monitoring of binding events on a thermostabilized human A2A receptor embedded in a lipid bilayer by surface plasmon resonance. *Biochim Biophys Acta* 2015, 1848:1224-1233.
31. Jamshad M, Charlton J, Lin YP, Routledge SJ, Bawa Z, Knowles TJ, Overduin M, Dekker N, Dafforn TR, Bill RM, et al. G-protein coupled receptor solubilization and purification for biophysical analysis and functional studies, in the total absence of detergent. *Biosci Rep* 2015, 35.
32. Whorton MR, Bokoch MP, Rasmussen SG, Huang B, Zare RN, Kobilka B, Sunahara RK. A monomeric G protein-coupled receptor isolated in a high-density lipoprotein particle efficiently activates its G protein. *Proc Natl Acad Sci U S A* 2007, 104:7682-7687.
33. Whorton MR, Jastrzebska B, Park PS, Fotiadis D, Engel A, Palczewski K, Sunahara RK. Efficient coupling of transducin to monomeric rhodopsin in a phospholipid bilayer. *J Biol Chem* 2008, 283:4387-4394.
34. Ernst OP, Gramse V, Kolbe M, Hofmann KP, Heck M. Monomeric G protein-coupled receptor rhodopsin in solution activates its G protein transducin at the diffusion limit. *Proc Natl Acad Sci U S A* 2007, 104:10859-10864.
35. Fanelli F, Fellingline A. Dimerization and ligand binding affect the structure network of A(2A) adenosine receptor. *Biochim Biophys Acta* 2011, 1808:1256-1266.
36. Burgueno J, Blake DJ, Benson MA, Tinsley CL, Esapa CT, Canela EI, Penela P, Mallol J, Mayor Jr. F, Lluís C, et al. The Adenosine A2a Receptor Interacts with the Actin-binding Protein alpha-Actinin. *Journal of Biological Chemistry* 2003, 278:37545-37552.
37. Ciruela F, Burgueno J, Casado V, Canals M, Marcellino D, Goldberg SR, Bader M, Fuxe K, Agnati LF, Lluís C, et al. Combining Mass Spectrometry and Pull-Down Techniques for the Study of Receptor Heteromerization. Direct Epitope-Epitope Electrostatic Interactions between Adenosine A2a and Dopamine D2 Receptors. *Analytical Chemistry* 2004, 76:5354-5363.
38. Lohse MJ, Nuber S, Hoffmann C. Fluorescence/bioluminescence resonance energy transfer techniques to study G-protein-coupled receptor activation and signaling. *Pharmacol Rev* 2012, 64:299-336.
39. Adamson RJ, Watts A. Kinetics of the early events of GPCR signalling. *FEBS Lett* 2014, 588:4701-4707.
40. Patching SG. Surface plasmon resonance spectroscopy for characterisation of membrane protein-ligand interactions and its potential for drug discovery. *Biochim Biophys Acta* 2014, 1838:43-55.
41. Altenbach C, Kusnetzow AK, Ernst OP, Hofmann KP, Hubbell WL. High-resolution distance mapping in rhodopsin reveals the pattern of helix movement due to activation. *Proc Natl Acad Sci U S A* 2008, 105:7439-7444.
42. Edwards DT, Huber T, Hussain S, Stone KM, Kinnebrew M, Kaminker I, Matalon E, Sherwin MS, Goldfarb D, Han S. Determining the oligomeric structure of proteorhodopsin by Gd<sup>3+</sup> - based pulsed dipolar spectroscopy of multiple distances. *Structure* 2014, 22:1677-1686.

43. Stone KM, Voska J, Kinnebrew M, Pavlova A, Junk MJ, Han S. Structural insight into proteorhodopsin oligomers. *Biophys J* 2013, 104:472-481.
44. Yang J, Aslimovska L, Glaubitz C. Molecular dynamics of proteorhodopsin in lipid bilayers by solid-state NMR. *J Am Chem Soc* 2011, 133:4874-4881.
45. Clements JM, Catlin GH, Price MJ, Edwards RM. Secretion of human epidermal growth factor from *Saccharomyces cerevisiae* using synthetic leader sequences. *Gene* 1991, 106:267-272.
46. Parekh R, Forrester K, Witttrup D. Multicopy Overexpression of Bovine Pancreatic Trypsin Inhibitor Saturates the Protein Folding and Secretory Capacity of *Saccharomyces cerevisiae*. *Protein Expr Purif* 1995, 6:537-545.
47. Bryksin AV, Matsumura I. Overlap extension PCR cloning: a simple and reliable way to create recombinant plasmids. *Biotechniques* 2010, 48:463-465.
48. Gietz RD, Woods RA. Yeast transformation by the LiAc/SS Carrier DNA/PEG method. *Methods Enzymol* 2002, 350:87-96.
49. O'Malley MA, Naranjo AN, Lazarova T, Robinson AS. Analysis of adenosine A(2)a receptor stability: effects of ligands and disulfide bonds. *Biochemistry* 2010, 49:9181-9189.
50. Weiss HM, Grisshammer R. Purification and characterization of the human adenosine A2a receptor functionally expressed in *Escherichia coli*. *European Journal of Biochemistry* 2002, 269:82-92.
51. Slotboom DJ, Duurkens RH, Olieman K, Erkens GB. Static light scattering to characterize membrane proteins in detergent solution. *Methods* 2008, 46:73-82.
52. White JF, Grodnitzky J, Louis JM, Trinh LB, Shiloach J, Gutierrez J, Northup JK, Grisshammer R. Dimerization of the class A G protein-coupled neurotensin receptor NTS1 alters G protein interaction. *Proc Natl Acad Sci U S A* 2007, 104:12199-12204.
53. Wen J, Arakawa T, Philo JS. Size-exclusion Chromatography with On-line Light-Scattering, Absorbance, and Refractive Index Detectors for Studying Proteins and Their Interactions. *Analytical Biochemistry* 1996, 240:155-166.
54. O'Malley MA, Helgeson ME, Wagner NJ, Robinson AS. Toward rational design of protein detergent complexes: determinants of mixed micelles that are critical for the in vitro stabilization of a G-protein coupled receptor. *Biophys J* 2011, 101:1938-1948.
55. Rath A, Glibowicka M, Nadeau VG, Chen G, Deber CM. Detergent binding explains anomalous SDS-PAGE migration of membrane proteins. *Proc Natl Acad Sci U S A* 2009, 106:1760-1765.
56. Lukasiqicz S, Blasiak E, Gorecka-Faron A, Polit A, Tworzydło M, Gorecki A, Wasylewski Z, Dziedzicka-Wasylewska M. Fluorescence studies of homooligomerization of adenosine A2A and serotonin 5-HT1A receptors reveal the specificity of receptor interactions in the plasma membrane. *Pharmacological Reports* 2007, 59:379-392.
57. De Filippo E, Namasivayam V, Zappe L, El-Tayeb A, Schiedel AC, Muller CE. Role of extracellular cysteine residues in the adenosine A receptor. *Purinergic Signal* 2016.
58. Naranjo AN, Chevalier A, Cousins GD, Ayyetey E, McCusker EC, Wenk C, Robinson AS. Conserved disulfide bond is not essential for the adenosine A2A receptor: Extracellular cysteines influence receptor distribution within the cell and ligand-binding recognition. *Biochim Biophys Acta* 2015, 1848:603-614.
59. Strop P, Brunger AT. Refractive index-based determination of detergent concentration and its application to the study of membrane proteins. *Protein Sci* 2005, 14:2207-2211.
60. Byron O, Vestergaard B. Protein-protein interactions: a supra-structural phenomenon demanding trans-disciplinary biophysical approaches. *Curr Opin Struct Biol* 2015, 35:76-86.
61. Briddon SJ, Gandia J, Amaral OB, Ferre S, Lluís C, Franco R, Hill SJ, Ciruela F. Plasma membrane diffusion of G protein-coupled receptor oligomers. *Biochim Biophys Acta* 2008, 1783:2262-2268.
62. Maslennikov I, Kefala G, Johnson C, Riek R, Choe S, Kwiatkowski W. NMR spectroscopic and analytical ultracentrifuge analysis of membrane protein detergent complexes. *BMC Struct Biol* 2007, 7:74.

63. Thevenin D, Lazarova T. Stable interactions between the transmembrane domains of the adenosine A2A receptor. *Protein Sci* 2008, 17:1188-1199.
64. Thevenin D, Lazarova T, Roberts MF, Robinson CR. Oligomerization of the fifth transmembrane domain from the adenosine A2A receptor. *Protein Sci* 2005, 14:2177-2186.
65. Gurevich VV, Gurevich EV. How and why do GPCRs dimerize? *Trends Pharmacol Sci* 2008, 29:234-240.
66. Johnston JM, Wang H, Provasi D, Filizola M. Assessing the relative stability of dimer interfaces in G protein-coupled receptors. *PLoS Comput Biol* 2012, 8:e1002649.
67. Guo W, Shi L, Filizola M, Weinstein H, Javitch JA. Crosstalk in G protein-coupled receptors: changes at the transmembrane homodimer interface determine activation. *Proc Natl Acad Sci U S A* 2005, 102:17495-17500.